

Interval-Based Diagnosis of Biological Systems - Application to an Anaerobic Digestion Pilot Plant

R. H. López-Bañuelos* V. Alcaraz-González^{*,**}
J. P. Steyer^{**} H. O. Méndez-Acosta* V. González-Álvarez*
C. Pelayo-Ortiz*

* *Departamento de Ingeniería Química, CUCEI-Universidad de Guadalajara Blvd. M. García Barragán 1451, C.P. 44430 Guadalajara, Jal, México*

** *INRA, UR050, Laboratoire de Biotechnologie de l'Environnement, Avenue des Etangs, Narbonne, F-11100, France*

Abstract: Anaerobic digestion is a highly nonlinear time-varying process used for biological wastewater treatment which is subject to large disturbances of both influent concentrations and flow rates. These perturbations can lead to the crash of the digester and thus, the dynamics of the main state variables - including biomass - must be closely monitored to use this information in the design and implementation of advanced control schemes. However, such processes still suffer from a lack of reliable and cheap sensors. As a consequence, efficient monitoring, control and decision support systems are needed in order to insure the correct process operation. Particularly, there is an increasing interest on the proposal of Fault Detection and Isolation (FDI) and Fault Detection and Analysis (FDA) integrated systems. In this paper, we propose the use of interval observers in order to detect and isolate sensor faults as well as input changes in biological systems that are not observable. This approach is experimentally implemented on a $1m^3$ pilot scale anaerobic digestion continuous process. *Copyright © 2008 IFAC*

1. INTRODUCTION

Anaerobic Digestion (AD) is a very complex biological process for wastewater treatment in which the Chemical Organic Demand (COD) from an influent is degraded into a gas mixture made of Carbon Dioxide (CO_2) and methane (CH_4) called biogas. The AD process is able to operate under severe conditions: high strength effluents and short hydraulic retention times. Furthermore, it has been experimentally demonstrated that this process is well adapted for urban and food wastewater treatment system.

One of the great challenges nowadays in AD is to lead the process towards a safe operation while improving its overall yield. However, it is well known that the presence of unknown disturbances may cause irreversible destabilization conditions leading to the crash of the AD process. In order to avoid this situation, several advanced control and supervision schemes have been developed in the last decade [Steyer et al., 2002, 2006]. Nevertheless, most of these schemes have found limited success since they depend on the availability of on-line information of key process variables that may be plagued by noise and time delays or simply are the result of a state estimation scheme from other measurements [Rapaport and Harmand, 2002]. Moreover, such schemes are designed on the basis that the AD process is fault-free, a situation that is rarely met in industry. In fact, actual AD processes are subject to a large number of faults, e.g., i) faults of sensors and actuators (e.g. disconnections, false contact), ii) unexpected changes on the process inputs (normally considered as perturba-

tions), etc. Thus, in order to guarantee proper AD process operation new but highly efficient Fault Detection and Diagnosis (FDD) strategies are needed.

Some studies on the supervision and the diagnosis of AD processes have been reported: see for instance [Steyer et al., 1997], [Genovesi et al., 2000] or [Lardon et al., 2004] and related references. Particularly, most of reported model-based diagnosis techniques have involved a strict characterization of noises and disturbances of the plants of interest, which is not a simple task. In any wastewater treatment process, the variations of the composition of the effluents to be treated are indeed badly known or uncertain. Thus, it is usually not possible to guarantee any stability or performance properties if actual input disturbances differ significantly from those of their nominal or initial characterization. Furthermore, in the presence of input uncertainties, most of classical estimation schemes cannot be implemented.

In order to compensate this observability handicap, interval observers (IO) have been recently proposed [Gouze et al., 2000, Alcaraz-González and González-Álvarez, 2007]. Interval observers are used to reconstruct guaranteed dynamical bounds on the unmeasured variables, (in the presence of process input uncertainties), instead of reconstructing their exact value. In fact, the design of an IO is based on the structure of any classical observer (an observer that can be designed if the inputs are known) and the additional condition that the error dynamics system is cooperative. This property ensures that, given a dynamical

system, two sets of initial conditions ordered term-by-term and some lower and upper bounds on the inputs in which the actual inputs may actually vary, then the solutions of this dynamical systems are also ordered. Particularly, the use of the well known asymptotic observer in the IO design is particularly suitable since it allows the user to deal at the same time with the nonlinearities of the systems, the unknown input disturbances and, in a more general sense, with any disturbance or uncertainty that can be considered as an unknown process input [Alcaraz-González and González-Alvarez, 2007].

Using an IO's set, Steyer et al. [2000] have designed an approach capable to detect and isolate faults in sensors as well as in the hypotheses used for the designing of observers and controllers. Such an approach is based on the construction of certain residuals which are calculated as the difference between the estimated and the measured variables, and they permit, in a simple but highly efficient way, the detection of faults and their origin in the AD process. In this paper, the system proposed by Steyer et al. [2000] is experimentally tested. The paper is organized as follows. First, the model of the process of interest, is presented. Then, the fault detection and the diagnosis approach is described. The IO's used for the residual generation are introduced and their use is highlighted with respect to the diagnosis objectives. Then, the approach is applied and experimentally implemented in a $1m^3$ pilot scale up-flow fixed bed anaerobic digester used for the treatment of red wine distillery wastewater in the Narbonne, France, area. Finally, experimental results are shown and discussed before some conclusions are drawn.

2. THE NONLINEAR MODEL

The biological scheme of the AD involves several multi-substrate multi-organism reactions that are performed both in series and in parallel (see for example [Henze and Harremoës, 1983]). The following is an AD process carried out in a continuous fixed bed reactor for the treatment of industrial wine distillery wastewater is considered [Bernard et al., 2001]:

$$\begin{aligned}
 \dot{X}_1 &= (\mu_1 - \alpha D)X_1 \\
 \dot{X}_2 &= (\mu_2 - \alpha D)X_2 \\
 \dot{Z} &= (Z^{in} - Z) \\
 \dot{S}_1 &= D(S_1^{in} - S_1) - k_1\mu_1 X_1 \\
 \dot{S}_2 &= D(S_2^{in} - S_2) + k_2\mu_1 X_1 - k_3\mu_2 X_2 \\
 \dot{C}_{TI} &= D(C_{TI}^{in} - C_{TI}) + k_7(k_8 P_{CO_2} + Z - C_{TI} - S_2) \\
 &\quad + k_4\mu_1 X_1 + k_5\mu_2 X_2
 \end{aligned} \tag{1}$$

where X_1 , X_2 , S_1 , S_2 , Z and C_{TI} are, respectively, the concentrations of acidogenic bacteria, methanogenic bacteria, COD, volatile fatty acids (VFA), strong ions and total inorganic carbon. P_{CO_2} is the CO_2 partial pressure. α , $0 \leq \alpha \leq 1$ is assumed constant and denotes the biomass fraction which is retained by the reactor bed, i.e. $\alpha = 0$, for the ideal fixed-bed reactor and $\alpha = 1$ for the ideal continuous stirred tank reactor. D is the dilution rate. The specific growth rate μ_1 and μ_2 are given by

$$\begin{aligned}
 \mu_1 &= \mu_{max1} S_1 / (K_{S1} + S_1) \\
 \mu_2 &= \mu_{max2} S_2 / [K_{S2} + S_2 + (S_2 / K_{I2})^2]
 \end{aligned}$$

which are the main causes of the strongly non-linear kinetic behavior of the model. The parameters definition and their values are listed in Table 1. In all cases, the upper index i indicates *influent concentrations*.

Two versions are possible for (1). The difference between these two versions is the expression for the dynamics of C_{TI} . In the first version, this expression is a P_{CO_2} function, exactly as in (1) whereas in the second one, it is a function of the gaseous CO_2 flow rate, Q_{CO_2} . Thus, it is possible to establish the next relation:

$$k_7(k_8 P_{CO_2} + Z - C_{TI} - S_2) = Q_{CO_2} / k_9 V,$$

where $k_9 = RT/P_T$ and V is the total volume in the reactor.

Now, let us consider the following definition for the state variables:

$$x_1 = X_1 \quad x_2 = X_2 \quad x_3 = Z \quad x_4 = C_{TI} \quad x_5 = S_1 \quad x_6 = S_2$$

Then, following this notation, the two versions of system (1) mentioned above are represented in matricial form by (2a) and (2b).

Table 1. Model parameters

Par	Meaning	Value
k_1	Yield coefficient for COD degradation	42.14 g COD/g X_1
k_2	Yield coefficient for fatty acid production	116.5 mmolVFA/g X_1
k_3	Yield coefficient for fatty acid consumption	268 mmolVFA/g X_2
k_4	Yield coefficient for CO_2 production due to X_1	50.6 mmol CO_2 /g X_1
k_5	Yield coefficient for CO_2 production due to X_2	343.6 mmol CO_2 /g X_2
k_6	Yield coefficient for CH_4 production	315 mmol CH_4 /g X_2
k_7	liquid/gas transfer rate	200 day^{-1}
k_8	Henry's constant	26.7 mmol CO_2 /lt-atm
α	Proportion of dilution rate for bacteria	0.5 (dimensionless)
μ_{max1}	Maximum acidogenic biomass growth rate	1.2 day^{-1}
μ_{max2}	Maximum methanogenic biomass growth rate	0.74 day^{-1}
K_{S1}	Saturation parameter associated with S_1	4.949 g COD/l
K_{S2}	Saturation parameter associated with S_2	9.28 mmol VFA/l
K_{I2}	Inhibition constant associated with S_2	16 (mmolVFA/l) $^{1/2}$
P_T	Total pressure in the reactor	1.0434 atm
V	Total volume in the reactor	0.948 m^3
T	Temperature in the reactor	38°C

3. FAULT DETECTION AND DIAGNOSIS

For the evaluation of the FDD system proposed in this work, six on-line measurements are available: S_1 , S_2 , C_{TI} , Z , Q_{CO_2} and P_{CO_2} . Our objective is to detect and isolate any possible sensor fault that may occur in a real

$$\begin{bmatrix} \dot{x}_1 \\ \dot{x}_2 \\ \dot{x}_3 \\ \dot{x}_4 \\ \dot{x}_5 \\ \dot{x}_6 \end{bmatrix} = \begin{bmatrix} 1 & 0 \\ 0 & 1 \\ 0 & 0 \\ k_4 & k_5 \\ -k_1 & 0 \\ k_2 & -k_3 \end{bmatrix} \begin{bmatrix} \mu_1 x_1 \\ \mu_2 x_2 \end{bmatrix} + \begin{bmatrix} -\alpha D & 0 & 0 & 0 & 0 & 0 \\ 0 & -\alpha D & 0 & 0 & 0 & 0 \\ 0 & 0 & -D & 0 & 0 & 0 \\ 0 & 0 & k_7 & -(D+k_7) & 0 & -k_7 \\ 0 & 0 & 0 & 0 & -D & 0 \\ 0 & 0 & 0 & 0 & 0 & -D \end{bmatrix} \begin{bmatrix} x_1 \\ x_2 \\ x_3 \\ x_4 \\ x_5 \\ x_6 \end{bmatrix} + \begin{bmatrix} Dx_1^{in} \\ Dx_2^{in} \\ Dx_3^{in} \\ Dx_4^{in} + k_7 k_8 P_{CO_2} \\ Dx_5^{in} \\ Dx_6^{in} \end{bmatrix} \quad (2a)$$

$$\begin{bmatrix} \dot{x}_1 \\ \dot{x}_2 \\ \dot{x}_3 \\ \dot{x}_4 \\ \dot{x}_5 \\ \dot{x}_6 \end{bmatrix} = \begin{bmatrix} 1 & 0 \\ 0 & 1 \\ 0 & 0 \\ k_4 & k_5 \\ -k_1 & 0 \\ k_2 & -k_3 \end{bmatrix} \begin{bmatrix} \mu_1 x_1 \\ \mu_2 x_2 \end{bmatrix} + \begin{bmatrix} -\alpha D & 0 & 0 & 0 & 0 & 0 \\ 0 & -\alpha D & 0 & 0 & 0 & 0 \\ 0 & 0 & -D & 0 & 0 & 0 \\ 0 & 0 & 0 & -D & 0 & 0 \\ 0 & 0 & 0 & 0 & -D & 0 \\ 0 & 0 & 0 & 0 & 0 & -D \end{bmatrix} \begin{bmatrix} x_1 \\ x_2 \\ x_3 \\ x_4 \\ x_5 \\ x_6 \end{bmatrix} + \begin{bmatrix} Dx_1^{in} \\ Dx_2^{in} \\ Dx_3^{in} \\ Dx_4^{in} - Q_{CO_2}/k_9 V \\ Dx_5^{in} \\ Dx_6^{in} \end{bmatrix} \quad (2b)$$

process on these variables as well as the detection of perturbations upon any of the four considered process input concentrations: $S_1^{in}, S_2^{in}, C_{ti}^{in}, Z^{in}$ which are considered as unmeasured. Such as perturbations may be detected as a violation of the following inequality:

$$u_i^{in-} \leq u_i^{in} \leq u_i^{in+} \quad (3)$$

where u_i^{in} is any of the concentration variables in the influent and the subscripts " + " and " - " indicate upper and lower bounds, respectively. In this last situation, the objective is to detect that the real process input violates its pre-specified lower or upper bounds. These hypotheses are not only required for the construction of the IO but they are also used in the design of robust control laws for this process [Alcaraz-González and González-Alvarez, 2007], which stands out once again the usefulness of detecting any unmeasured perturbation upon these variables. The next subsection shows the interval observer which was used for building some residuals on the measured variables.

3.1 Interval observers

Consider the following general nonlinear time varying lumped model:

$$\dot{\mathbf{x}}(t) = \mathbf{C}\mathbf{f}(\mathbf{x}(t), t) + \mathbf{A}(t)\mathbf{x}(t) + \mathbf{b}(t) \quad (4)$$

where $\mathbf{x}(t) \in \mathbb{R}^n$ is the state vector, $\mathbf{f}(\mathbf{x}(t), t) \in \mathbb{R}^r$ denotes the vector of nonlinearities and $\mathbf{C} \in \mathbb{R}^{n \times r}$ represents a matrix of constant coefficients. The time varying matrix $\mathbf{A}(t) \in \mathbb{R}^{n \times n}$ is the state matrix while $\mathbf{b}(t) \in \mathbb{R}^n$ gathers inputs and/or other possibly time varying functions. The state space may be split in such a way that (4) can be rewritten as:

$$\begin{aligned} \dot{\mathbf{x}}_1 &= \mathbf{C}_1 \mathbf{f}(\mathbf{x}(t), t) + \mathbf{A}_{11}(t) \mathbf{x}_1(t) + \mathbf{A}_{12}(t) \mathbf{x}_2(t) + \mathbf{b}_1(t) \\ \dot{\mathbf{x}}_2 &= \mathbf{C}_2 \mathbf{f}(\mathbf{x}(t), t) + \mathbf{A}_{21}(t) \mathbf{x}_1(t) + \mathbf{A}_{22}(t) \mathbf{x}_2(t) + \mathbf{b}_2(t) \end{aligned} \quad (5)$$

where the $\mathbf{x}_2(t)$ vector gathers the m measured state variables and $\mathbf{x}_1(t)$ represents the variables that have to be estimated. Matrices $\mathbf{A}_{11}(t) \in \mathbb{R}^{s \times s}$, $\mathbf{A}_{12}(t) \in \mathbb{R}^{s \times m}$, $\mathbf{A}_{21}(t) \in \mathbb{R}^{m \times s}$, $\mathbf{A}_{22}(t) \in \mathbb{R}^{m \times m}$, $\mathbf{C}_1 \in \mathbb{R}^{s \times r}$, $\mathbf{C}_2 \in \mathbb{R}^{m \times r}$, $\mathbf{b}_1 \in \mathbb{R}^s$ and $\mathbf{b}_2 \in \mathbb{R}^m$ are the corresponding partitions of $\mathbf{A}(t)$, \mathbf{C} and $\mathbf{b}(t)$, respectively.

Let us recall the following result:

Lemma 1. Let $\dot{\zeta} = \mathbf{f}(\zeta, t) + \mathbf{g}(t)$. This system is said to be a cooperative system if $\partial \mathbf{f}_i(\zeta, t) / \partial \zeta_j \geq 0, \forall i \neq j$. It implies that if $\mathbf{g}(t) \geq 0 \forall t \geq 0$, then $\zeta(t) \geq 0, \forall t \geq 0$. The proof of this lemma can be found in [Smith, 1995]. In (4), some

bounds are available for the initial conditions and $\mathbf{b}(t)$ is assumed to be unmeasured, but within known lower and upper bounds. In such a situation, notice that (4) may be no longer observable. Consequently, it is not possible to design a classical observer like the asymptotic observer. Nevertheless, we can use its basic stable structure and its property of being independent of the nonlinearities, to design a robust set-valued observer in order to build guaranteed intervals for the unmeasured variables instead of estimating them precisely, provided that the Lemma 1 holds. Thus, the following dynamic system:

$$\left. \begin{aligned} & \text{For the upper bound:} \\ & \dot{\mathbf{w}}^+(t) = \dot{\mathbf{W}}^+(t) \mathbf{w}^+(t) + \mathbf{X}(t) \mathbf{x}_2(t) + \mathbf{M} \mathbf{v}^+(t) \\ & \mathbf{w}(0)^+ = \mathbf{N} \mathbf{x}(0)^+ \\ & \hat{\mathbf{x}}_1^+(t) = \mathbf{N}_1^{-1} (\mathbf{w}^+(t) - \mathbf{N}_2 \mathbf{x}_2(t)) \\ & \text{For the lower bound:} \\ & \dot{\mathbf{w}}^-(t) = \dot{\mathbf{W}}^-(t) \mathbf{w}^-(t) + \mathbf{X}(t) \mathbf{x}_2(t) + \mathbf{M} \mathbf{v}^-(t) \\ & \mathbf{w}(0)^- = \mathbf{N} \mathbf{x}(0)^- \\ & \hat{\mathbf{x}}_1^-(t) = \mathbf{N}_1^{-1} (\mathbf{w}^-(t) - \mathbf{N}_2 \mathbf{x}_2(t)) \end{aligned} \right\} \quad (6)$$

with $\mathbf{M} = [\mathbf{N}_1; \mathbf{N}_2; \tilde{\mathbf{N}}_2], \tilde{\mathbf{N}}_2 = \llbracket \mathbf{N}_2, ij \rrbracket$,

$$\mathbf{v}^+(t) = [\mathbf{b}_1^+(t) \ 1/2(\mathbf{b}_2^+(t) + \mathbf{b}_2^-(t)) \ 1/2(\mathbf{b}_2^+(t) - \mathbf{b}_2^-(t))]^T,$$

$$\mathbf{v}^-(t) = [\mathbf{b}_1^-(t) \ 1/2(\mathbf{b}_2^+(t) + \mathbf{b}_2^-(t)) \ -1/2(\mathbf{b}_2^+(t) - \mathbf{b}_2^-(t))]^T$$

where $\mathbf{W}(t) = (\mathbf{N}_1 \mathbf{A}_{11}(t) + \mathbf{N}_2 \mathbf{A}_{21}(t)) \mathbf{N}_1^{-1}$, $\mathbf{X}(t) = \mathbf{N}_1 \mathbf{A}_{12}(t) + \mathbf{N}_2 \mathbf{A}_{22}(t) - \mathbf{W}(t) \mathbf{N}_2$, $\mathbf{N}_1 \in \mathbb{R}^{s \times s}$, is an arbitrary invertible matrix, $\mathbf{N}_2 = -\mathbf{N}_1 \mathbf{C}_1 \mathbf{C}_2^\perp$ with $\mathbf{N}_2 \in \mathbb{R}^{s \times r}$, \mathbf{C}_2^\perp is the generalized pseudo-inverse of \mathbf{C}_2 and

$\mathbf{N} = [\mathbf{N}_1; \mathbf{N}_2]$; is a stable robust interval observer for (4) independent of the nonlinearities $\mathbf{f}(\mathbf{x}(t), t)$ [Alcaraz-González and González-Alvarez, 2007].

In our application it is possible to build five interval observers. Due to the lack of space, their explicit form is not shown here, but all of them follow the same design structure showed in (6). However, their main design features are summarized in Table 2:

3.2 The residuals

In this work, three kinds of residuals were considered and generated. a) the difference between the measurement

Table 2. Interval observers

Observer	Measurements	Estimated bounds for	Model version
Ob1	—	Z	1
Ob2	S_1 and S_2	CTI	1
Ob3	S_2 and CTI	S_1	2
Ob4	S_2 and CTI	X_2	1
Ob5	S_2 and CTI	X_2	2

and its estimate (upper and/or lower), b) the difference between the measurement and its model prediction and c) the difference between two estimates generated by two different observers.

For the state variables S_1 , CTI and Z , it is possible to design an observer that yields upper and lower estimated bounds. Then, the respective residuals are constructed as the difference between the measurements and the estimated bounds. Figure 1 shows the input CTI and their guessed bounds. Figures 2 to 4 represent the comparison between the measured variable and its estimated for S_1 , CTI and Z respectively.

In the case of the state variable S_2 , any interval observer with the structure of (6) mets the Lemma 1. Then, it is not possible to have an interval observer for this variable. We thus consider faults in the S_2 sensor when the difference between the measured state and the model prediction is higher than a certain threshold (e.g. 5 mmol/l). Figure 5 shows the comparison between measurements for S_2 and its model prediction. For PCO_2 and QCO_2 , we assume that the sensors do not have important failures in the considered time interval. However, in order to test the robustness of the proposed approach when facing possible measurement errors, we have considered these two measured variables into a threshold given by a $\pm 5\%$ confidence interval.

From the observers defined before, it is possible to generate a total of 7 residuals for this application. The observers Ob1, Ob2 and Ob3 were used to generated 6 residuals, while the observers Ob4 and Ob5 were used to generate a last residual ($r_{4/5}(\hat{X}_2^+)$) which compares the upper and lower bounds of the same variable X_2 . For further details about the creation of the residuals and the evaluation process of them see [Steyer et al., 2000, Alcaraz-González and González-Alvarez, 2007]

$$\begin{aligned}
 Ob1 : & \left\{ \begin{array}{l} r^+(1) = \hat{Z}^+(t) - Z(t) \\ r^-(1) = Z(t) - \hat{Z}^-(t) \end{array} \right\} \text{ fault if } \left\{ \begin{array}{l} r^+(1) < 0 \\ \text{or} \\ r^-(1) < 0 \end{array} \right\} \\
 Ob2 : & \left\{ \begin{array}{l} r^+(2) = \hat{C}_{TI}^+(t) - C_{TI}(t) \\ r^-(2) = C_{TI}(t) - \hat{C}_{TI}^-(t) \end{array} \right\} \text{ fault if } \left\{ \begin{array}{l} r^+(2) < 0 \\ \text{or} \\ r^-(2) < 0 \end{array} \right\} \\
 Ob3 : & \left\{ \begin{array}{l} r^+(3) = \hat{S}_1^+(t) - S_1(t) \\ r^-(3) = S_1(t) - \hat{S}_1^-(t) \end{array} \right\} \text{ fault if } \left\{ \begin{array}{l} r^+(3) < 0 \\ \text{or} \\ r^-(3) < 0 \end{array} \right\} \\
 Ob4\&5 : r_{(4/5)}(\hat{X}_2^+) = |\hat{X}_2^+(4) - \hat{X}_2^+(5)|, \text{ fault if } r_{(4/5)}(\hat{X}_2^+) > \varepsilon
 \end{aligned}$$

3.3 On the signatures

Residuals $r^+(1)$ to $r^-(1)$, when they are negative, highlight essentially the fact that the measurement of the

Table 3. Signatures table

residuals activation	$Z - PCO_2$	$Z - CTI$	$Z - S_2$	S_{1in}^+	S_{1in}^-
$r^+(1)$	1/0	1/0	1/0	0	0
$r^-(1)$	0/1	0/1	0/1	0	0
$r^+(2)$	1/0	1/0	1/0	1	0
$r^-(2)$	0/1	0/1	0/1	0	1
$r^+(3)$	0	1/0	1/0	1	0
$r^-(3)$	0	0/1	0/1	0	1
$r_{4/5}$	1	1	1	0	0

residuals activation	S_1	S_2	Z	CTI	PCO_2	QCO_2
$r^+(1)$	0	0	1/0	0	0	0
$r^-(1)$	0	0	0/1	0	0	0
$r^+(2)$	1/0	1/0	0	1/0	1/0	0
$r^-(2)$	0/1	0/1	0	0/1	0/1	0
$r^+(3)$	1/0	1/0	0	1/0	0	1/0
$r^-(3)$	0/1	0/1	0	0/1	0	0/1
$r_{4/5}$	0	1	1	1	1	1
	S_{2in}^+	S_{2in}^-	Z_{in}^+	Z_{in}^-	C_{TIin}^+	C_{TIin}^-
$r^+(1)$	0	0	1	0	0	0
$r^-(1)$	0	0	0	1	0	0
$r^+(2)$	1	0	1	0	1	0
$r^-(2)$	0	1	0	1	0	1
$r^+(3)$	1	0	0	0	1	0
$r^-(3)$	0	1	0	0	0	1
$r_{4/5}$	0	0	0	0	0	0

respective substrate concentration in the reactor exists out of their lower and upper estimated bounds. Thus, in order to determine the presence of a fault, it is simply enough to check the sign of the residual. On the other hand, the residual $r_{4/5}$ is compared with a threshold fixed by the user. Notice also that for these residuals only one of each pair may be activated (upper or lower) if a fault occurs. This is the explanation of notations 1/0 and 0/1 in Table(3). Then, if it is kept in mind that a fault on a variable would activate only a certain number of residuals, then the combination of active and inactive residuals would be, in principle unique for each kind or fault. The residuals obtained above are able to create the corresponding signature for the fault detection in each variable. In other words, to each variable it corresponds a kind of fingerprint or signature, which is a function of the residuals and is a suitable tool to detect the fault that may occur on such a variable.

In this work, we use an extension of the table used in [Steyer et al., 2000]. We consider the cases where simultaneous faults for the pairs Z and PCO_2 , Z and CTI and Z and S_2 occur (see Table 3). Notice that the signatures for the pairs $Z - CTI$ and $Z - S_2$ are identical and that the simultaneous detection for these combinations is possible only when the faults are effectively present and there is not any other fault in none of the rest of the variables at the same time interval. Under these considerations Table (3) includes the combination of signatures for the faults of $Z - PCO_2$, $Z - CTI$ and $Z - S_2$.

4. SIMULATION RESULTS AND DISCUSSION

Simulations were carried out off-line with the data obtained from a $1m^3$ up-flow fixed-bed anaerobic digester used for the treatment of red wine vinasses which is located

in Narbonne, France. The DDF approach was experimentally implemented off-line. However, the theoretical framework depicted above as well as the excellent results shown here suggest that a true on-line implementation may be easily carried out. Experiments were carried out over 37 days in which several faults occurred (see Table 4).

Table 4. Faults to consider

Fault N°	Time (d)	Affected variable(s)
1	5.209 - 5.234	S_1
2	5.966 - 5.985	S_1
3	8.112 - 10.921	Z
4	12.826 - 12.856	Z and C_{TI}
5	13.523 - 13.602	Z
6	14.020 - 15.000	S_2
7	14.208 - 15.000	Z
8	18.385 - 18.550	Z and C_{TI}
9	18.550 - 18.775	Z and C_{TI}
10	18.775 - 18.818	Z and C_{TI}
11	18.875 - 20.100	Z and C_{TI}
12	20.114 - 20.164	Z
13	21.132 - 21.233	Z
14	26.847 - 26.867	Z and C_{TI}
15	26.867 - 27.000	Z
16	27.000 - 27.312	C_{TI}
17	27.829 - 27.924	Z and C_{TI}
18	27.924 - 27.980	Z
19	33.000 - 34.500	S_2
20	33.1200 - 33.180	Z
21	533.212 - 33.268	Z
22	33.953 - 33.994	Z
23	34.100 - 34.800	Z
24	35.000 - 39.000	C_{TIin}
25	39.100 - 39.151	Z and C_{TI}
26	39.151 - 39.209	Z and C_{TI}
27	39.209 - 39.227	Z and C_{TI}
28	39.227 - 39.928	Z and C_{TI}
29	40.965 - 41.900	C_{TIin}
30	41.085 - 41.276	Z and C_{TI}

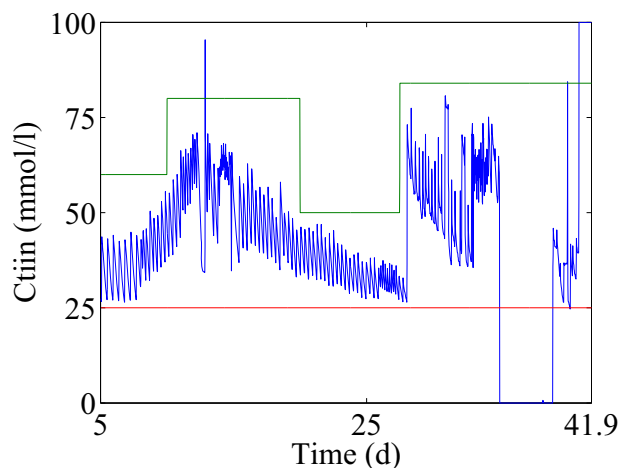


Fig. 1. Lower, upper and real C_{TI}^{in} (mmol/l)

Figure 6 depicts the most significant result in this paper since it is here where the FDD system is synthesized. From the lower line to the upper line, they are the FDD representation for Z , P_{CO_2} , Q_{CO_2} , $Z - C_{TI}$ ($Z - S_2$) and $Z - P_{CO_2}$ respectively. From this figure, we can deduce the following: As it is seen, the FDD system was able to detect

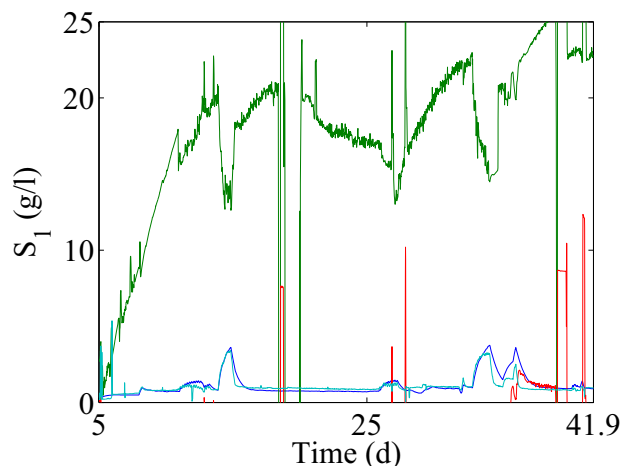


Fig. 2. Lower and upper bounds, estimated and real S_1 .

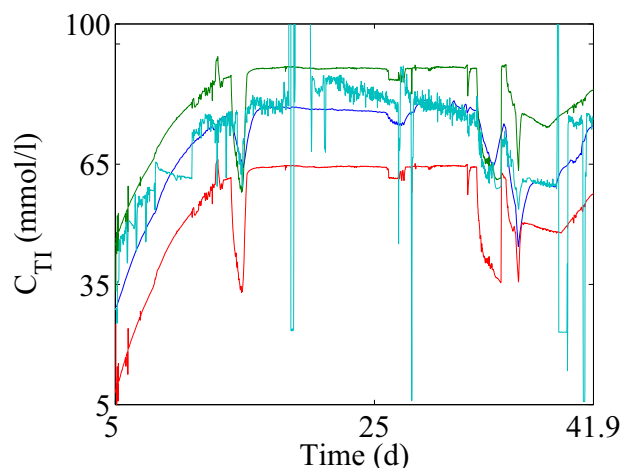


Fig. 3. Lower and upper bounds, estimated and real C_{TI} (mmol/).

and isolate correctly the faults 3, 5, 7, 12, 13, 15, 18, 20, 21, 22, 23 which correspond to the variable Z (see Figure 1), as well as the faults 4, 8, 9, 10, 11, 14, 17, 25, 26, 27, 28 and 30 which correspond to the pair $Z - C_{TI}$. The faults 1, 2 and 24 were detected exactly although they were not isolated in the correct line in the figure, since the faults are not high enough for that C_{TI} to cross the bounds computed for the observer Ob2. Similar results were obtained for the faults 6, 16 and 19; they were detected correctly but not isolated in the correct line in the figure. The most likely cause of these results is the fact that the faults had practically no effect on the corresponding residuals (r^3) to be detected. It is also clear that the fault 29 was not detected since it is not an actual fault but a lack of information in the validation. A number of false-alarms (FA) exists. These FA are due to a slow convergence of the observers, which produce that the residuals may be activated or not for the timely detection. Notice however, that these FA disappear once the residuals have converged.

5. CONCLUSIONS

The Interval-based FDD approach proposed in this paper was able to detect most of the faults occurring in the actual

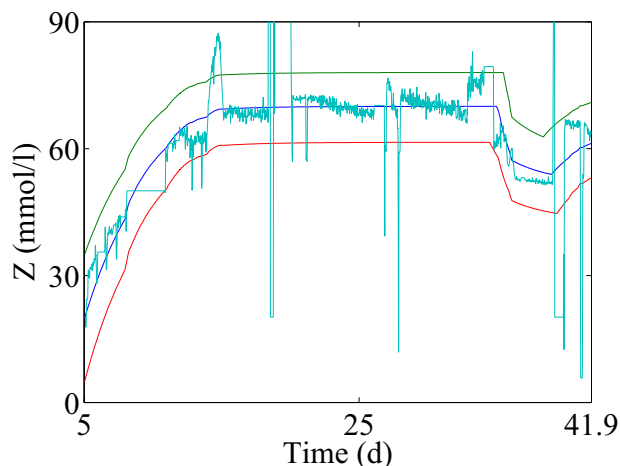


Fig. 4. Lower and upper bounds, estimated and real concentration for Z (mmol/l).

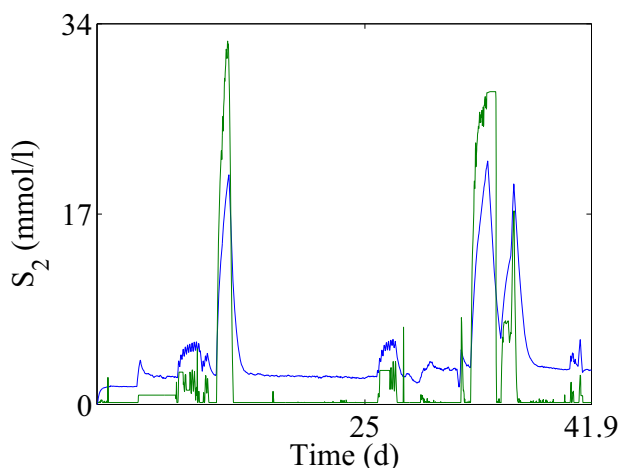


Fig. 5. Estimate and measurements for S_2 (mmol/l).

anaerobic digestion wastewater treatment process used to experimentally validate the approach. In particular, it showed optimal results for the fault detection and isolation on the variable Z . The proposed approach was also able to detect and isolate simultaneous faults for several variables. Even in the presence of some false alarms, the proposed approach was capable to detect up to 95% of the faults and to isolate up to 75% of them.

REFERENCES

- V. Alcaraz-González and V. González-Alvarez. *Selected topics in dynamics and control of chemical and biological processes*, chapter Robust nonlinear observer for bioprocesses: Application to wastewater treatment, pages 125–172. Springer, Berlin, 2007.
- O. Bernard, Z. Hadj-Sadok, D. Dochain, A. Genovesi, and J.P. Steyer. Dynamical model development and parameter identification for anaerobic wastewater treatment process. *Biotechnol. Bioeng.*, 75(4):424–438, 2001.
- A. Genovesi, J. Harmand, and J.P. Steyer. Integrated Fault Detection and Isolation: Application to a Winery's Wastewater Treatment Plant. *Applied Intelligence*, 13(1):59–76, 2000.

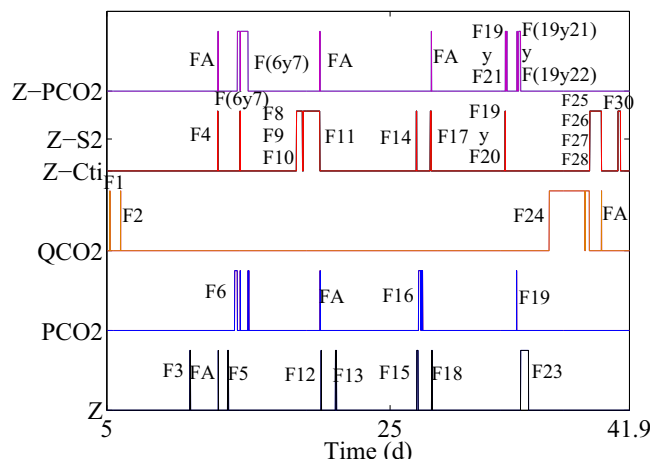


Fig. 6. Fault detection and isolation of the considered faults

- JL Guze, A. Rapaport, and MZ Hadj-Sadok. Interval observers for uncertain biological systems. *Ecological Modelling*, 133(1):45–56, 2000.
- M. Henze and P. Harremoës. Anaerobic treatment of wastewater in fixed film reactors: a literature review. *Water science and technology*, 15(8/9), 1983.
- L. Lardon, A. Punal, and JP Steyer. On-line diagnosis and uncertainty management in biological wastewater treatment processes. *Journal of Process Control*, 14: 747–763, 2004.
- A. Rapaport and J. Harmand. Robust regulation of a class of partially observed nonlinear continuous bioreactors. *Journal of Process Control*, 12(2):291–302, 2002.
- H.L Smith. Monotone dynamics systems: an introduction to the theory of competitive and cooperative systems. *Mathematical surveys and monographs*, 41:31–53, 1995.
- J.P. Steyer, D. Rolland, J.C. Bouvier, and R. Moletta. Hybrid fuzzy neural network for diagnosis-application to the anaerobic treatment of wine distillery wastewater in a fluidized bed reactor. *Water Science and Technology*, 36(6):209–217, 1997.
- JP Steyer, J. Harmand, and V. Alcaraz-Gonzales. Interval based diagnosis of an anaerobic digester pilot plant. *Proceedings*, pages 174–179, 2000.
- J.P. Steyer, J.C. Bouvier, T. Conte, P. Gras, and P. Sousbie. Evaluation of a four year experience with a fully instrumented anaerobic digestion process. *Wat. Sci. Technol.*, 45(4-5):495–502, 2002.
- J.P. Steyer, O. Bernard, D.J. Batstone, and I. Angelidaki. Lessons learnt from 15 years of ICA in anaerobic digesters. *Wat. Sci. Technol.*, 53(4):25–33, 2006.